Rotamerism, Tautomerism, and Excited-State Intramolecular Proton Transfer in 2-(4′-*N*,*N*-Diethylamino-2′-hydroxyphenyl)benzimidazoles: Novel Benzimidazoles Undergoing Excited-State Intramolecular Coupled Proton and Charge Transfer

Sonia Ríos Vázquez, M. Carmen Ríos Rodríguez,* Manuel Mosquera, and Flor Rodríguez-Prieto*

Departamento de Química Física, Facultade de Química, Universidade de Santiago de Compostela, E-15782 Santiago de Compostela, Spain

Received: August 17, 2007; In Final Form: October 16, 2007

The solvent and temperature dependence of the phototautomerization of 1-methyl-2-(2′-hydroxyphenyl)-benzimidazole (**4**) and the novel compounds 2-(4′-amino-2′-hydroxyphenyl)benzimidazole (**1**), 2-(4′-*N*,*N*-diethylamino-2′-hydroxyphenyl)benzimidazole (**2**), and 1-methyl-2-(4′-*N*,*N*-diethylamino-2′-hydroxyphenyl)-benzimidazole (**3**), together with the ground-state rotamerism and tautomerism of these new compounds, have been studied by UV−vis absorption spectroscopy and steady-state and time-resolved fluorescence spectroscopy. A solvent-modulated rotameric and tautomeric equilibrium is observed in the ground state for **1**, **2**, and **3**. In cyclohexane, these compounds mainly exist as a planar syn normal form, with the hydroxyl group hydrogen-bonded to the benzimidazole N3. In ethanol, the syn form is in equilibrium with its planar anti rotamer (for **1** and **2**), with the phenyl ring rotated 180° about the C2−C1′ bond and with a nonplanar rotamer for compound **3**. In aqueous solution, a tautomeric equilibrium is established between the anti normal form (or the nonplanar rotamer for **3**) and the tautomer (with the hydroxyl proton transferred to the benzimidazole N3). The syn normal form of these compounds undergoes in all the solvents an excited-state intramolecular proton-transfer process from the hydroxyl group to the benzimidazole N3 to yield the excited tautomer. The tautomer fluorescence quantum yield of **2**, **3**, and **4** shows a temperature-, polarity-, and viscosity-dependent radiationless deactivation, connected with a large-amplitude conformational motion. We conclude that this excited-state conformational change experienced by the tautomer is associated with an intramolecular charge transfer from the deprotonated dialkylaminophenol or phenol (donor) to the protonated benzimidazole (acceptor), affording a nonfluorescent charge-transfer tautomer. Therefore, these compounds undergo an excited-state intramolecular coupled proton- and charge-transfer process.

Introduction

The coupling between charge transfer and proton motion is far from being understood[1] in spite of being essential in many processes occurring in living systems, such as DNA chemical damage and repair,[2] photostability of DNA base pairs and proteins,[3,4] cellular respiration,[5,6] and photosynthesis.[7] We have recently reported[8] that some *o*-hydroxyarylbenzazoles undergo a proton-coupled charge transfer. In particular, for these molecules an excited-state intramolecular proton-transfer (ESIPT) process induces an intramolecular charge migration.

ESIPT is observed in molecules with an acid and a basic site in a suitable conformation to form an intramolecular hydrogen bond and is due to the increase of acidity and/or basicity of these groups upon excitation.[9,10] ESIPT molecules have applications as UV photostabilizers,[11] photoswitches,[12] or fluorescent probes[13] and are potential materials for organic light-emitting diodes.[14] Among such molecules are 2-(2′-hydroxyphenyl)benzimidazole (HBI),[9,10,15−22] 2-(2′-hydroxyphenyl)-benzoxazole (HBO),[9,10,15,23−28] 2-(2′-hydroxyphenyl)benzothiazole (HBT),[9,10,15,22,29−34] 2-(3′-hydroxy-2′-pyridil)benzimidazole (HPyBI),[35] and 2-(3′-hydroxy-2′-pyridil)benzoxazole (HPyBO)[8] (Chart 1).

CHART 1: Structures of Various Species Showing ESIPT. The Normal Forms (N_{syn} and N_{anti} Conformers) and the Tautomeric Forms (T_{syn} and T_{anti} Conformers) Are Shown

	HBI	HBO	HBT	HPyBI	HPyBO
X	NH	O	S	NH	O
Y	CH	CH	CH	N	N

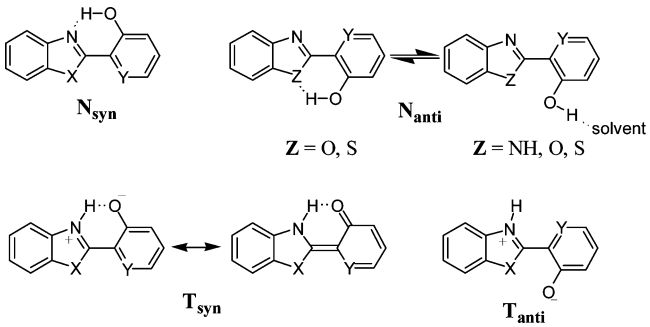

The most stable form of the mentioned ESIPT molecules in the ground state is the planar syn normal form $\mathbf{N_{syn}}$ (Chart 1), with the hydroxyl group hydrogen-bonded to the benzazole N3. Upon excitation, $\mathbf{N_{syn}}$ undergoes an ultrarapid ESIPT from the hydroxyl group to the benzazole N3 to yield the tautomer $\mathbf{T^*_{syn}}$, with large Stokes shifted fluorescence, no emission from the

* Authors to whom correspondence should be addressed. M. C. Ríos Rodríguez: qfcaryrr@usc.es, F. Rodríguez-Prieto: qfflorrp@usc.es.

10.1021/jp076634a CCC: $40.75
Published on Web 12/23/2007

syn normal form being detected. In protic solvents, a rotameric equilibrium in the ground state exists (except for HPyBI) between $\mathbf{N_{syn}}$ and its anti rotamer $\mathbf{N_{anti}}$, without the N···H−O intramolecular hydrogen bond (Chart 1). The $\mathbf{N_{anti}}$ rotamer of the benzoxazole and benzothiazole derivatives may also experience a conformational equilibrium between an intramolecularly hydrogen-bonded conformer (with O···HO or S···HO hydrogen bond) and the OH-rotated conformer, hydrogen-bonded to the solvent (Chart 1). This equilibrium of the $\mathbf{N_{anti}}$ form is not possible for the benzimidazole derivatives, as the intramolecular hydrogen bond cannot be formed with the NH group. Both $\mathbf{N_{anti}}$ rotamers are unable to undergo ESIPT and give normal **N*** fluorescence upon excitation.

In aqueous solution, ground-state HPyBI exhibits a tautomeric equilibrium between $\mathbf{N_{syn}}$ and **T**, whereas a ground-state rotameric and tautomeric equilibrium between $\mathbf{N_{syn}}$, $\mathbf{N_{anti}}$, and **T** is established for HBI and HPyBO. In spite of the similar structures of these hydroxyarylbenzazoles, the fluorescence quantum yields of their tautomers showed remarkable differences. Whereas the fluorescence quantum yield of **T*** was for HBI and HPyBI essentially independent of solvent and temperature, the values for HBO, HPyBO, and HBT were much lower than those of HBI and HPyBI and experienced a viscosity- and temperature-dependent radiationless deactivation attributed to a large-amplitude conformational motion. Furthermore, for both HBO and HBT in apolar solvents, the anti tautomer $\mathbf{T_{anti}}$ (Chart 1) was detected[36−41] after excitation as a transient ground-state species, suggesting that the excited-state conformational motion undergone by the tautomer of these compounds is a syn−anti (usually called cis−trans) isomerization[36,37,41,42] that would lead to a more stable $\mathbf{T^*_{anti}}$ rotamer. This isomerization is precluded for HBI and HPyBI, as their tautomer is symmetrical.

We have recently shown[8] that the large-amplitude motion undergone by **T*** is connected to an intramolecular charge migration from the deprotonated phenol or pyridinol (donor) to the protonated benzazole (acceptor), this yielding a nonfluorescent charge-transfer intermediate $\mathbf{T^*_{CT}}$, and that HBI and HPyBI do not experience this excited-state intramolecular coupled proton and charge transfer because their tautomers do not contain an adequate electron donor−acceptor pair for the process to occur. To further support our interpretation of the results, we decided to investigate hydroxyphenylbenzimidazoles bearing a better electron donor (an amino or dialkylamino group at C4′, compounds **1** and **2**; Chart 2) to test if they undergo a similar proton-coupled charge-transfer process to that described for HPyBO, HBO, HBT, and their derivatives. Moreover, as the intramolecular charge migration is associated with a large-amplitude motion that could involve rotation around the interannular bond, we also investigated derivatives of HBI with a methyl group at the benzimidazole N1 (compounds **3** and **4**), as the greater steric hindrance should favor the rotation and therefore the charge-transfer process.

In this paper, we present the results for the ground- and excited-state behavior of the novel ESIPT benzimidazoles 2-(4′-diamino-2′-hydroxyphenyl)benzimidazole (**1**), 2-(4′-*N*,*N*-diethylamino-2′-hydroxyphenyl)benzimidazole (**2**), and 1-methyl-2-(4′-*N*,*N*-diethylamino-2′-hydroxyphenyl)benzimidazole (**3**) in different solvents. We report the room-temperature fluorescence of these new compounds in solvents of various viscosities and polarities and investigate the temperature dependence of the fluorescence of **2** and **3** in diethyl ether, 1-methyl-2-(2′-hydroxyphenyl)benzimidazole **4** in diethyl ether and butyronitrile, and HBI in 2-butanol.

CHART 2: Molecular Structures of the Compounds Studied in This Work

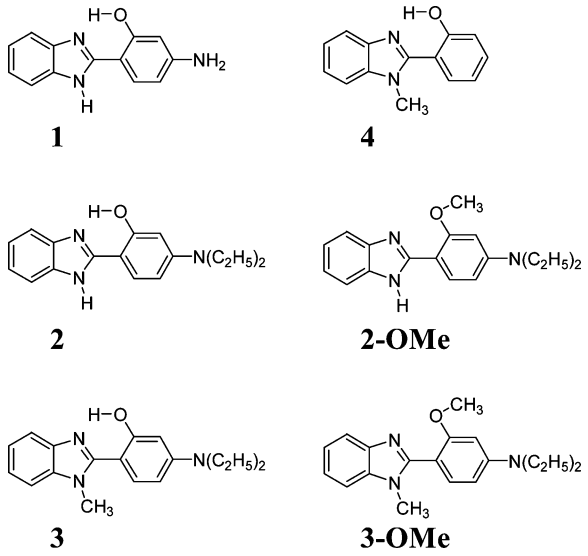

The main objectives of this work are (1) to investigate the influence of the dialkylamino group at C4′ in both the ESIPT process and the ground-state rotamerism and tautomerism of the HBI derivatives and (2) to study if a temperature-dependent radiationless deactivation process of the excited tautomer, associated with a large-amplitude conformational motion and a charge migration, occurs for these benzimidazoles. The model compounds 2-(4′-*N*,*N*-diethylamino-2′-methoxyphenyl)benzimidazole (**2-OMe**) and 1-methyl-2-(4′-*N*,*N*-diethylamino-2′-methoxyphenyl)benzimidazole (**3-OMe**), unable to give ESIPT, were also studied.

Experimental Section

Materials. HBI[21] and **4**[43] were synthesized as described elsewhere.

Compound **1** was prepared by reaction in the dark of 25 mmol of 1,2-benzenediamine (Aldrich) with 40 mmol of 4-amino-2-hydroxy-benzoic acid (Aldrich) in refluxing toluene for 36 h in the presence of 80 mmol of PCl_3. The product was purified by sublimation. The solutions of **1** were highly unstable, this fact preventing the characterization of the product obtained and also the determination of the fluorescence lifetimes, which required a long measurement time. We could only measure the spectra of **1** solutions, as they could be recorded in a short time. A fresh solution was always prepared for measuring each of the spectra.

Compound **2** was obtained by heating a mixture of 15 mmol of 4-diethylamino-2-hydroxy-benzaldehyde (Aldrich) with 15 mmol of 1,2-benzenediamine (Aldrich) in 15 mL of nitrobenzene for 3 days at ∼50 °C. The product was purified by sublimation. ^{1}H NMR (300 MHz, $CDCl_3$), δ (ppm): 1.19 (t, 6H, t, $J = 7.1$ Hz), 3.37 (c, 4H, $J = 7.1$ Hz), 6.26 (dd, 1H, $J = 8.8$ Hz, $J = 2.5$ Hz), 6.34 (d, 1H, $J = 2.5$ Hz), 7.22 (dd, 2H, $J = 5.9$ Hz, $J = 3.1$ Hz), 7.39 (d, 1H, $J = 8.8$ Hz), 7.53 (m, 2H). MS, *m*/*z* (relative intensity): 281 (59.2, M), 266 (100, M − 15), 238 (27.7, M − 43).

To synthesize the derivative **2-OMe**, we previously prepared 4-diethylamino-2-methoxy-benzaldehyde by adding 60 mmol of MeI dropwise over a solution of 15 mmol of 4-diethylamino-2-hydroxy-benzaldehyde (Aldrich) in 40 mmol of dimethylsulfoxide (DMSO) basified with 60 mmol of KOH. **2-OMe** was synthesized by heating a solution of 10 mmol of 4-diethylamino-

2-methoxy-benzaldehyde with 10 mmol of 1,2-benzenediamine (Aldrich) in 50 mL of ethanol at ~50 °C for 4 days. The product was recrystallized from ethanol. ^{1}H NMR (300 MHz, $CDCl_3$), δ (ppm): 1.23 (t, 6H, $J = 7.1$ Hz), 3.34 (c, 4H, $J = 7.1$ Hz), 4.05 (s, 3H), 6.24 (d, 1H, $J = 2.3$ Hz), 6.44 (dd, 1H $J = 8.9$ Hz, $J = 2.3$ Hz), 7.19 (dd, 2H, $J = 5.8$ Hz, $J = 3.1$ Hz), 7.60 (m, 2H), 8.37 (d, 1H, $J = 8.9$ Hz). MS, *m*/*z* (relative intensity): 295 (100, M), 280 (88.5, M − 15), 250 (47.5, M − 45).

Compound **3** was prepared by refluxing for 2 days a mixture of 15 mmol of 4-diethylamino-2-hydroxy-benzaldehyde (Aldrich) and 15 mmol of *N*-methyl-1,2-benzenediamine (Aldrich) in 40 mL of ethanol under O_2 flow. The product was precipitated from the reaction mixture by adding water. ^{1}H NMR (300 MHz, $CDCl_3$), δ (ppm): 1.22 (t, 6H, $J = 7.1$ Hz), 3.40 (c, 4H, $J = 7.1$ Hz), 3.99 (s, 3H), 6.29 (dd, 1H, $J = 8.9$ Hz, $J = 2.6$ Hz), 6.40 (d, 1H, $J = 2.6$ Hz), 7.26 (dd, 2H, $J = 5.9$ Hz, $J = 3.0$ Hz), 7.33 (m, 1H, $J = 1.6$ Hz, $J = 3.0$ Hz, $J = 5.9$ Hz), 7.58 (d, 1H, $J = 8.9$ Hz), 7.68 (dd, 1H, $J = 5.9$ Hz, J=3.0 Hz). MS, *m*/*z* (relative intensity): 295 (69.1, M), 280 (100.0, M − 15), 266 (22.0, M − 29), 250 (23.0, M − 45).

Derivative **3-OMe** was obtained by adding 1.8 mmol of MeI dropwise to a solution of 0.3 mmol of **2** in 10 mL of DMSO previously basified with 1.2 mmol of KOH. The product was recrystallized from ethanol. ^{1}H NMR (300 MHz, $CDCl_3$), δ (ppm): 1.22 (t, 6H, $J = 7.1$ Hz), 3.41 (c, 4H, $J = 7.1$ Hz), 3.65 (s, 3H), 3.79 (s, 3H), 6.24 (d, 1H, $J = 2.1$ Hz), 6.38 (dd, 1H, $J = 8.5$ Hz, $J = 2.1$ Hz), 7.23 (m, 2H), 7.34 (m, 1H), 7.41 (d, 1H, $J = 8.5$ Hz), 7.77 (m, 1H). MS, *m*/*z* (relative intensity): 309 (47.2, M), 294 (35.3, M − 15), 278 (19.4, M − 31), 206 (100.0, M − 103).

Methods. Solutions were made up in double-distilled water and spectroscopy-grade solvents and were not degassed. Acidity, in aqueous solutions, was varied with NaH_2PO_4/Na_2HPO_4 buffer (made up with Merck p.a. products). The pH of the aqueous solutions was chosen so that no protonated or deprotonated forms were present in appreciable concentrations. Sample concentrations of $\sim 10^{-5}$ mol dm^{-3} for absorption and $\sim 10^{-6}$ mol dm^{-3} for fluorescence were employed. All experiments were carried out at 25 °C except otherwise stated.

pH was measured with a Radiometer PHM 82 pH meter equipped with a Radiometer Type B combined electrode. UV−vis absorption spectra were recorded in a Varian Cary 3E spectrophotometer. Fluorescence excitation and emission spectra were recorded in a Spex Fluorolog-2 FL340 E1 T1 spectrofluorometer, with correction for instrumental factors by means of a Rhodamine B quantum counter and correction files supplied by the manufacturer. UV−vis absorption and fluorescence measurements at low temperature were performed using an Oxford Instruments liquid nitrogen cryostat model 1704 with an ITC 503 control unit, and the spectra obtained were corrected for the temperature dependence of the solution volume. Fluorescence quantum yields were measured using quinine sulfate ($< 3 \times 10^{-5}$ mol dm^{-3}) in aqueous H_2SO_4 (0.5 mol dm^{-3}) as a standard ($\phi = 0.546$).[44,45]

Fluorescence lifetimes were determined by single-photon timing in an Edinburgh Instruments FL-900 spectrometer equipped with a hydrogen-filled nanosecond flashlamp and the reconvolution analysis software supplied by the manufacturer. The estimated uncertainty of the lifetime measurements is about 0.1 ns. The lifetime values collected in the tables below show typically a smaller standard deviation because we report the values obtained in the fitting procedures, without corrections for additional causes of errors. The reported lifetime standard deviations give only information about the quality of the fits.

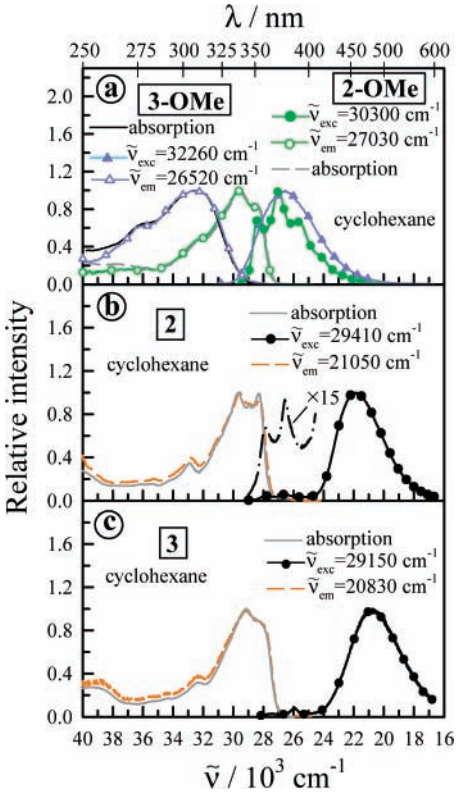

Figure 1. Normalized fluorescence excitation and emission spectra of (a) **2-OMe** and **3-OMe**, (b) **2**, and (c) **3** in cyclohexane together with the absorption spectra in the same solvent.

Model equations were fitted to the experimental data by means of a nonlinear weighted least-squares routine based on the Marquardt algorithm. The reported uncertainties of the parameters represent the statistical standard deviations obtained in the fitting procedures.

Results

Absorption, Fluorescence Spectra, and Lifetimes of 1, 2, 3, 2-OMe, and 3-OMe in Various Solvents. *Aprotic Solvents.* The fluorescence spectra of the methoxy derivatives **2-OMe** and **3-OMe** were recorded in cyclohexane (Figure 1a). For both compounds, excitation and emission spectra were independent of the monitoring wavenumbers. A single emission band, peaking at about 27 000 cm^{-1}, was observed for both species (more structured for **2-OMe**), and the excitation spectrum matched the absorption spectrum measured in the same solvent. It can be observed that whereas for **2-OMe** the excitation band overlapped its emission spectrum that of **3-OMe** was strongly blue-shifted (Stokes shift 5900 cm^{-1}). The excitation and absorption maximum of **2-OMe** is 3300 cm^{-1} red-shifted with respect to that of **3-OMe**. The fluorescence quantum yields of the methoxy compounds in various solvents are listed in Table 1. The fluorescence decays were monoexponential for both compounds in all of the solvents studied (Table 2).

The fluorescence spectra of **2** and **3** in cyclohexane are shown in Figures 1b and 1c, together with the absorption spectra recorded in the same solvent. The fluorescence emission spectra of both compounds, peaking at ~21 000 cm^{-1}, showed an abnormally large Stokes shift with respect to its excitation spectrum, which coincides with the absorption spectrum. Furthermore, a very weak shoulder was observed in the emission spectrum at about 27 000 cm^{-1} (its intensity was too low to record the excitation spectrum), the position where their methoxy

TABLE 1: Tautomer Fluorescence Quantum Yields (ϕ_T) of HBI, 2, 3, and 4 and Those of the Normal Forms (ϕ_N) of 3, 2-OMe, and 3-OMe in Various Solvents for Which the Viscosity η and the Relative Dielectric Permittivity ϵ_r Are Shown

			ϕ_T				ϕ_N		
solvent	η^a/cP	$\epsilon_r{}^b$	HBI	2	3	4	3	2-OMe	3-OMe
diethyl ether	0.24	4.20		0.04	0.006	0.04			
acetonitrile	0.36	35.94	0.25	0.04	0.0007	0.01[d]		0.39	0.16
dichloromethane	0.42	8.93			0.002				0.12
methanol	0.55	32.66	0.15	0.07		0.02[c]		0.60	
cyclohexane	0.98	2.02	0.11	0.06	0.008	0.09[c]		0.26	0.11
ethanol	1.20	24.55		0.09		0.03[d]	0.25	0.37	0.22
dioxane	1.44	2.21				0.05[c]		0.32	0.17
ethylene glycol	19.90	37.70	0.16	0.12				0.57	

[a] Values at 298.15 K from ref 54. [b] Values at 298.15 K from ref 51. [c] From ref 20. [d] From ref 43.

TABLE 2: Fluorescence Decay Times τ of 2-OMe and 3-OMe in Various Solvents at 298 K

	2-OMe				3-OMe			
solvent	$\tilde{\nu}_{exc}$/cm^{-1}	$\tilde{\nu}_{em}$/cm^{-1}	τ/ns	χ^2	$\tilde{\nu}_{exc}$/cm^{-1}	$\tilde{\nu}_{em}$/cm^{-1}	τ/ns	χ^2
cyclohexane	29 410	25 000	1.194 ± 0.003	0.979				
	29 410	23 260	1.184 ± 0.003	0.967				
tetrahydrofuran	28 990	26 670	1.241 ± 0.002	1.036	31 750	25 970	0.603 ± 0.002	0.914
	28 990	23 810	1.232 ± 0.002	1.048	31 750	22 990	0.605 ± 0.002	1.100
acetonitrile	29 410	27 030	1.333 ± 0.002	1.050	31 650	25 970	0.617 ± 0.003	1.096
	29 410	23 810	1.327 ± 0.002	1.010	31 650	23 260	0.623 ± 0.003	1.061
ethylene glycol	29 410	25 640	1.406 ± 0.003	0.998	32 260	27 030	1.267 ± 0.003	1.064
	29 410	23 260	1.431 ± 0.003	1.059	32 260	23 260	1.199 ± 0.003	1.160
ethanol	28 990	26 320	1.331 ± 0.002	1.008	31 750	25 970	0.693 ± 0.003	1.110
	28 990	23 530	1.318 ± 0.002	0.953	31 750	22 220	0.685 ± 0.002	1.254
water, pH 8.50	29 410	24 390	1.437 ± 0.003	1.007				
	29 410	23 810	1.438 ± 0.003	1.063				

TABLE 3: Fluorescence Decay Times τ and Associated Percentages (in Parentheses) of 2 in Various Solvents at 298 K

solvent	$\tilde{\nu}_{exc}$/cm^{-1}	$\tilde{\nu}_{em}$/cm^{-1}	τ_1/ns	τ_2/ns	χ^2
tetrahydrofuran	29 410	22 730		0.793 ± 0.003	1.045
acetonitrile	28 570	26 320	1.39 ± 0.02 (66%)	0.39 ± 0.03 (34%)	1.100
	28 570	22 990	1.4[a] (10%)	0.325 ± 0.007 (90%)	1.032
	28 570	20 410	1.4[a] (9%)	0.310 ± 0.008 (91%)	1.037
ethylene glycol	29 410	27 400	1.388 ± 0.004		1.057
	29 410	24 390	1.39[a] (48%)	0.72 ± 0.01 (52%)	1.008
	29 410	23 260	1.39[a] (34%)	0.74 ± 0.01 (66%)	1.037
	29 410	22 220	1.39[a] (31%)	0.74 ± 0.01 (69%)	1.165
ethanol	30 770	25 970	1.291 ± 0.004		1.094
	29 410	25 000	1.28 ± 0.06 (60%)	0.65 ± 0.04 (40%)	0.999
	29 410	24 390	1.28[a] (24%)	0.65 ± 0.01 (76%)	1.065
	29 410	23 260	1.28[a] (11%)	0.67 ± 0.01 (89%)	1.086
	29 410	21 740	1.28[a] (11%)	0.639 ± 0.009 (89%)	1.140
water, pH 7.90	31 250	27 400	1.534 ± 0.005		1.167
	31 250	26 320	1.60 ± 0.02 (81%)	0.65 ± 0.08 (19%)	1.041
	31 250	25 000	1.651 ± 0.009 (82%)	0.6[a] (18%)	1.069
	31 250	23 810	1.74 ± 0.01 (70%)	0.6[a] (30%)	1.167

[a] Fixed.

derivatives fluoresce (Figure 1a). The fluorescence spectra of compound **1** (data not shown) were almost coincident with those of **2**.

The fluorescence quantum yields of **2** and **3** in cyclohexane and other solvents are compiled in Table 1. It is observed that the values in cyclohexane (0.06 for **2** and 0.008 for **3**) were much lower than those recorded for the methoxy analogues **2-OMe** (0.26) and **3-OMe** (0.11) in the same solvent. Fluorescence quantum yields and lifetimes could not be measured for **1** in any solvent studied, as this compound proved to be unstable under irradiation. Furthermore, as the fluorescence quantum yield of **3** was about 10 times lower than that of **2** and both compounds showed similar fluorescent behavior, the fluorescence decays were only recorded for **2**. A monoexponential decay was obtained for this compound in tetrahydrofuran (THF) with a decay time of 0.80 ns (Table 3). In acetonitrile, the fluorescence decay was however biexponential in the wavenumber range of 26 320−20 410 cm^{-1}. A decay time of 1.39 ns (mainly contributing at high wavenumbers) was obtained, together with a second decay time of ∼0.32 ns, its contribution to the fluorescence decay being higher at low wavenumbers.

Ethanol. The fluorescence spectra of **1** and **2** in ethanol are shown in Figures 2a and 2b, together with their absorption spectra in the same solvent. Dual fluorescence was observed for both compounds independently of the excitation wavenumber: an intense lower-energy (red) band (with maxima at 23 310 cm^{-1} for **1** and at 23 980 cm^{-1} for **2**), similar to the main emission band detected for **2** (and for **1**, spectra not shown) in cyclohexane (Figure 1b), accompanied by a weaker higher-energy (blue) band at ∼27 000 cm^{-1}. For both **1** and **2**, the main emission maximum showed a large Stokes shift with respect to the excitation spectrum, which almost coincided with the absorption spectrum. Moreover, the excitation spectrum recorded for **2** at the blue band (very similar to that obtained for **1**) almost matched the excitation spectrum of its methoxy derivative, **2-OMe**, in the same solvent (Figure 2b), and the

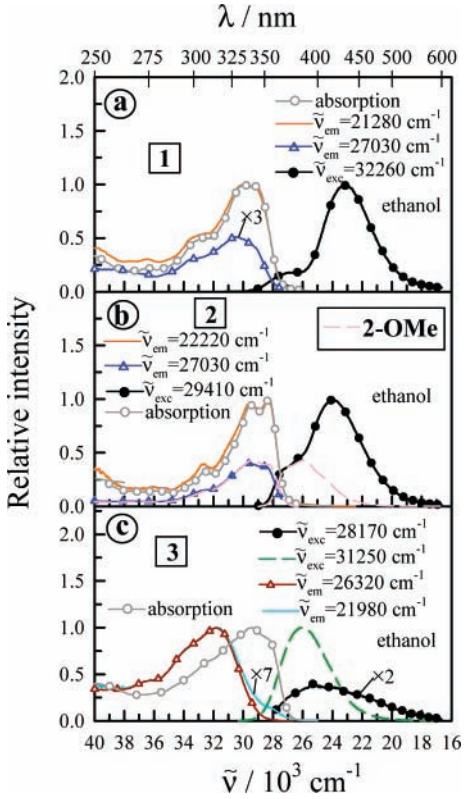

Figure 2. Normalized fluorescence excitation and emission spectra of (a) **1**, (b) **2** and **2-OMe** ($\tilde{\nu}_{exc}$ = 29 325 cm^{-1}, $\tilde{\nu}_{em}$ = 25 970 cm^{-1}), and (c) **3** in ethanol together with the absorption spectra in the same solvent.

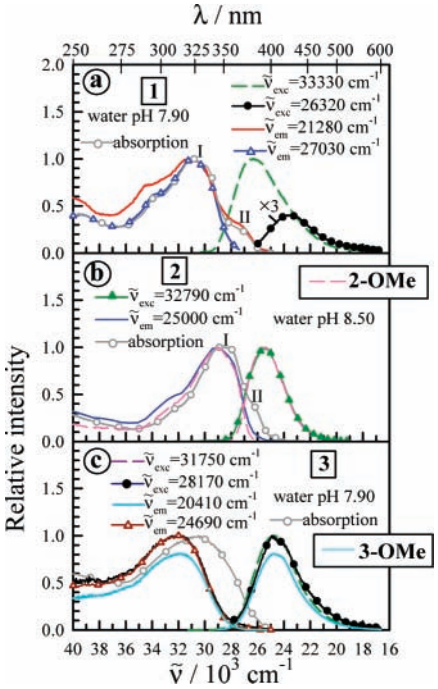

Figure 3. Normalized fluorescence excitation and emission spectra in an aqueous solution of (a) **1** at pH 7.90, (b) **2** and **2-OMe** at pH 8.50 (for the last compound, $\tilde{\nu}_{exc}$ = 29 070 cm^{-1}, $\tilde{\nu}_{em}$ = 25 640 cm^{-1}), and (c) **3** at pH 7.90 and **3-OMe** at pH 9.90 (for the last species, $\tilde{\nu}_{exc}$ = 31 750 cm^{-1}, $\tilde{\nu}_{em}$ = 25 000 cm^{-1}). The absorption spectra of **1**, **2**, and **3** in aqueous solution under the same acidity conditions are also plotted.

emission spectrum of **2-OMe** practically coincided with the blue fluorescence band of **2**. The fluorescence quantum yield of the red band of **2** in ethanol was estimated by subtracting from the global fluorescence the contribution of the blue band (its spectral shape assumed to be that of the emission spectrum of **2-OMe**), this leading to a value of 0.09 (Table 1). The fluorescence decay of **2** in ethanol was monoexponential at 25 970 cm^{-1} with a decay time of 1.29 ns (Table 3) and became biexponential at $\tilde{\nu}_{em} \leq$ 25 000 cm^{-1} with a decay time of 1.28 ns, showing its maximum contribution at high emission wavenumbers, and a second decay time of ∼0.65 ns, mainly contributing at low emission wavenumbers. The fluorescence quantum yield of **2-OMe** was measured to be 0.37 (Table 1), and the fluorescence decay was monoexponential with a decay time of 1.32 ns (Table 2).

The fluorescence spectra were also recorded for **3** (Figure 2c). A single emission band (maximum at 25 940 cm^{-1}, fluorescence quantum yield of 0.25), located at about the same position as that of the blue emission band of both **1** and **2**, was detected under excitation at 31 250 cm^{-1}. The excitation spectrum obtained at about the maximum of the emission band hardly overlapped its emission and did not coincide with the absorption spectrum (it was about 2300 cm^{-1} blue-shifted with respect to the absorption band). Moreover, under excitation at 28 170 cm^{-1} (close to the maximum of the absorption band), a very broad and weak fluorescence band, peaking at 25 350 cm^{-1}, was detected. The fluorescence spectra of **3-OMe** in ethanol (spectra not shown) were very similar to those obtained for this compound in water (Figure 3c). The fluorescence decay of **3-OMe** in ethanol was monoexponential (Table 2) with a decay time of 0.69 ns, and the fluorescence quantum yield (Table 1) was 0.22.

Aqueous Solution. The fluorescence spectra of **1** in aqueous solution are shown in Figure 3a, together with the absorption spectrum. The absorption showed an intense band (band I) at 31 000 cm^{-1} and a weaker band (band II) at ∼27 000 cm^{-1}. Upon excitation in absorption band II, an emission band (peaking at 23 720 cm^{-1}) very similar to that recorded in ethanol and cyclohexane and overlapping absorption band II was obtained. The excitation spectrum monitored at 21 280 cm^{-1} showed, like the absorption spectrum, bands I and II, but it did not match the absorption spectrum. Excitation of **1** at 33 330 cm^{-1} led to a different emission band, located at 26 280 cm^{-1}, its excitation spectrum lacking band II and overlapping the emission band.

The absorption spectrum of **2** in aqueous solution (Figure 3b) was very similar to that of **1**, showing bands I and II. The fluorescence emission spectrum (Figure 3b) showed only one band (located at 25 380 cm^{-1}), narrower than that recorded for **1** under the same conditions. Its excitation spectrum showed no contribution of band II, was slightly blue-shifted with respect to the absorption spectrum, and was very similar to the excitation band recorded for **1** under similar conditions. Furthermore, the excitation and emission bands of **2** almost coincided with those measured for the methoxy derivative **2-OMe** under the same conditions (Figure 3b). The fluorescence decay of **2-OMe** was monoexponential with a decay time of 1.44 ns. The fluorescence decay of **2** was monitored between 27 400 and 23 810 cm^{-1} under excitation in band I (Table 3). The fluorescence decay was monoexponential at 27 400 cm^{-1} with a decay time of 1.53 ns, whereas at $\tilde{\nu}_{em} \leq$ 26 000 cm^{-1} it became biexponential with a decay time of ∼1.65 ns, showing its maximum contribution at high wavenumbers, and a second decay time of 0.65 ns, contributing mainly at low wavenumbers.

The absorption spectrum of the N-methylated derivative **3** in aqueous solution, peaking at 30 500 cm^{-1}, was very broad

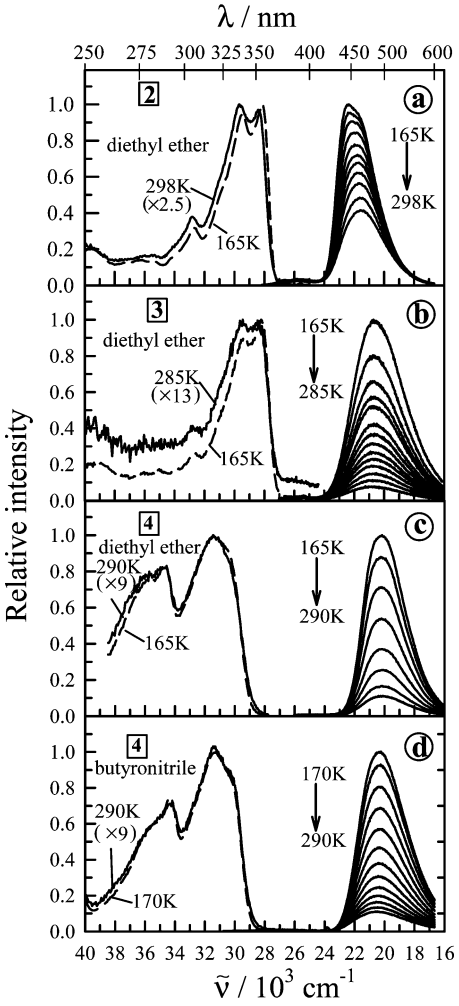

Figure 4. Fluorescence emission spectra of (a) **2** in diethyl ether in the temperature range of 165−298 K ($\tilde{\nu}_{exc}$ = 29 410 cm^{-1}) together with the normalized excitation spectra at 165 and 298 K ($\tilde{\nu}_{em}$ = 22 220 cm^{-1}), (b) **3** in diethyl ether in the temperature range of 165−285 K ($\tilde{\nu}_{exc}$ = 28 570 cm^{-1}) together with the normalized excitation spectra at 165 and 285 K ($\tilde{\nu}_{em}$ = 21 050 cm^{-1}), (c) **4** in diethyl ether in the temperature range of 165−290 K ($\tilde{\nu}_{exc}$ = 31 250 cm^{-1}) together with the normalized excitation spectra at 165 and 290 K ($\tilde{\nu}_{em}$ = 20 000 cm^{-1}), and (d) **4** in butyronitrile in the temperature range of 170−290 K ($\tilde{\nu}_{exc}$ = 31 250 cm^{-1}) together with the normalized excitation spectra at 170 and 290 K ($\tilde{\nu}_{em}$ = 20 830 cm^{-1}).

(Figure 3c). The spectrum o f **3-OMe** was narrower and blue-shifted (1600 cm^{-1}) with respect to that of **3**. The emission spectra of **3** and **3-OMe** (Figure 3c) were very similar. They showed a single band that shifted very slightly to the red on decreasing the excitation wavenumber for **3** and was independent of the excitation wavenumber for **3-OMe**. The excitation spectra were also very similar for both compounds, but whereas for **3-OMe** a perfect match of the excitation spectrum with the absorption spectrum was observed, for compound **3** the excitation spectrum was 1560 cm^{-1} blue-shifted with respect to the absorption spectrum. For both compounds, the fluorescence excitation and emission spectra hardly overlapped.

Influence of Temperature on the Fluorescence of HBI, 2, 3, and 4. The fluorescence spectra of compounds **2** and **3** were recorded in diethyl ether over a wide range of temperatures (Figures 4a and 4b). It is observed that the fluorescence intensity decreased 2.9 times for **2** and 13.4 times for **3** on increasing the temperature from 165 K to room temperature. The temperature dependence of the fluorescence spectra of **4** was studied in diethyl ether (Figure 4c) and in butyronitrile (Figure 4d).

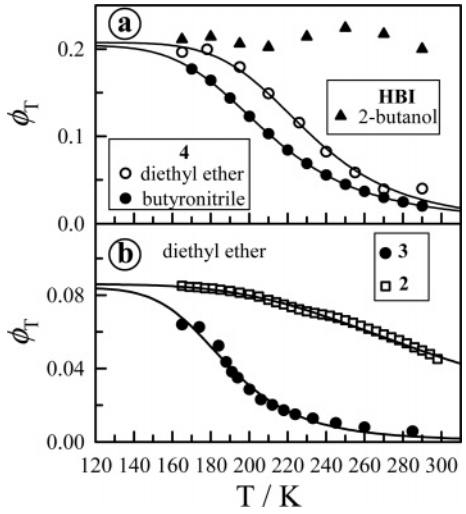

Figure 5. Temperature dependence of the tautomer fluorescence quantum yields ϕ_T of (a) HBI in 2-butanol and **4** in diethyl ether and butyronitrile (calculated from the fluorescence spectra of Figures 4c and 4d) together with the fit of eq 2 to the experimental data and (b) **2** and **3** in diethyl ether (calculated from the fluorescence spectra of Figures 4a and 4b) together with the fit of eq 2 to the experimental data.

The fluorescence quantum yield decreased drastically (9.3 times in butyronitrile and 9.0 times in diethyl ether) on increasing the temperature from 165−170 K to room temperature. Furthermore, it is seen in Figure 4 that, in both butyronitrile and diethyl ether, the excitation spectrum of **4** did not change in the temperature range studied, and those of **2** and **3** showed only a very slight blue shift on increasing the temperature. The temperature dependence of the fluorescence spectra of HBI in 2-butanol was also studied between 165 and 290 K (spectra not shown), no significant dependence being observed. The influence of temperature on the fluorescence quantum yields of these compounds is shown in Figure 5.

Discussion

Interpretation of the Absorption, Fluorescence Spectra, and Lifetimes of 1, 2, 3, 2-OMe, and 3-OMe in Various Solvents: ESIPT and Solvent-Modulated Ground-State Rotamerism and Tautomerism. *Aprotic Solvents.* For **2-OMe** and **3-OMe** (Figure 1a), both the excitation and the emission spectra were independent of the monitoring wavenumber, the excitation spectrum matched the absorption spectrum, and the fluorescence decay was monoexponential, indicating that only one species is present in both the ground and the excited states. For **2-OMe**, the excitation and emission bands overlapped, suggesting that the fluorescent species is the same as that being excited, that is, the normal form **N*** (probably a planar form in syn or anti conformation, the latter stabilized by an N−H···O hydrogen bond). Therefore, the fluorescence decay time (1.19 ns) and the fluorescence quantum yield (0.26) determined for **2-OMe** in cyclohexane correspond to **N***, both values showing no significant dependence on the solvent. The emission spectrum of **3-OMe** (Figure 1a) was located at about the same position as that of **2-OMe**, but the excitation and absorption spectra were about 3300 cm^{-1} blue-shifted with respect to **2-OMe**. This suggests that the fluorescent species are similar, but the ground-state structures differ for both compounds. The fact that the excitation and emission bands of **3-OMe** hardly overlapped indicates that for **3-OMe** the structure of the ground-state species is different from that of the fluorescent species. As **3-OMe** only differs from **2-OMe** in that **3-OMe** possesses a methyl group

at N1, we suggest that steric hindrance causes the normal form of **3-OMe** to be nonplanar in the ground state ($\mathbf{N_{np}}$), but upon excitation the molecule adopts a planar conformation. A similar behavior was previously found by us for the N1-methylated derivatives of HBI[43] and HPyBI.[46] The fluorescence quantum yield and lifetime values of **N*** (Tables 1 and 2) were for **3-OMe** about half of those found for **2-OMe**, but, as occurred with compound **2-OMe**, no clear dependence of these values on solvent polarity or viscosity was found.

The fluorescence spectral features of compounds **2** and **3** in cyclohexane (Figures 1b and 1c) were very similar. Both compounds showed a fluorescence emission band (peaking at ~21 000 cm^{-1}) that did not overlap the excitation band attributed to the normal form **N**. The unusually large Stokes shift observed indicates that the structure of the fluorescent species is not the same as that of the species being excited. Furthermore, the fact that for the derivatives **2-OMe** and **3-OMe**, with no hydroxyl group, only the emission band of **N*** was detected suggests that the excited-state process undergone by **2** and **3** is connected with the presence for both molecules of a hydroxyl group at C2′. We suggest that **2** and **3** experience a photoinduced intramolecular proton transfer to yield tautomer **T*** in a similar way as that reported for HBI[9,10,15−22] and its analogue HPyBI.[35] Furthermore, the formation of **T*** must be very rapid, as it could not be detected with our single-photon-counting equipment (time resolution ~0.1 ns). This indicates that the hydroxyl group must be hydrogen-bonded to the benzimidazole N3 already in the ground state, that is, in a planar "normal" syn (frequently named cis) conformation $\mathbf{N_{syn}}$ (Chart 1). A very weak structured emission at ~27 000 cm^{-1}, similar to that obtained for **2-OMe** (due to **N***), was observed for **2**, this suggesting the presence for this compound of a minor fraction of **N** molecules in the ground state without the intramolecular hydrogen bond N···H−O (and therefore unable to yield **T*** upon excitation). As the amount of this ground-state form unable to give ESIPT considerably increased in protic solvents, its conformation will be discussed later. However, the fluorescence decay time of **2** was monoexponential in THF with a decay time of 0.80 ns that must correspond to **T***. In acetonitrile, a biexponential decay was obtained (Table 3) with decay times of 1.4 and 0.32 ns. The short decay time showed its maximum contribution at the emission maximum of **T***, and therefore it must be due to the tautomer. Moreover, the long decay time almost coincided with that obtained for **2-OMe** (due to **N***) in the same solvent (1.33 ns) and showed its maximum contribution at about the emission maximum of **2-OMe**, indicating that it corresponds to the normal form **N***.

Ethanol. Because the fluorescence spectra of **1** and **2** showed the same general features in ethanol (Figures 2a and 2b), the behavior of both compounds in this solvent must be very similar. Therefore, we will mainly focus on compound **2**, the results being also valid for **1**. The fluorescence of **2** in ethanol shows two peaks. The main emission band and its excitation spectrum were very similar in shape and position to those obtained in cyclohexane (Figure 1b), attributed to **T*** and $\mathbf{N_{syn}}$, respectively, suggesting that **T*** is also the main fluorescing species for **2** (and **1**) in ethanol and that this excited species is formed by ESIPT after excitation of the $\mathbf{N_{syn}}$ conformer. However, the weak blue-shifted emission band detected for **2** in ethanol almost coincided with the fluorescence band recorded for its methoxy derivative (Figure 2b), attributed to **N***. The excitation spectrum at this blue band also matches the excitation spectrum of **2-OMe**, a compound for which an intramolecular hydrogen bond N··· H−O does not exist. Furthermore, the absorption spectrum of

SCHEME 1: Excitation and Deactivation Pathways of 1 (R = H) and 2 (R = C_2H_5) in Ethanol[a]

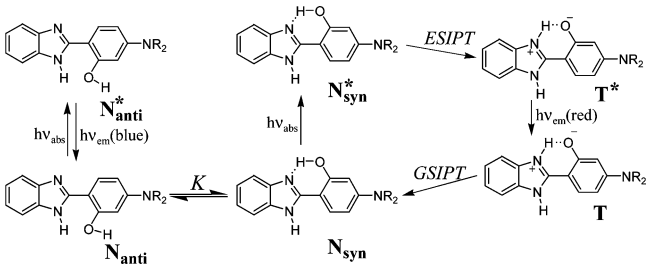

[a] The ground-state equilibrium between $\mathbf{N_{anti}}$ and $\mathbf{N_{syn}}$ strongly favors the latter.

2 almost coincided with the excitation spectrum of the red-shifted fluorescence band (Figure 2b), this indicating that $\mathbf{N_{syn}}$ is the main species present in the ground state. All this suggests that in ethanol **1** and **2** exist in the ground state in a conformational equilibrium between the normal form $\mathbf{N_{syn}}$, yielding **T*** upon excitation, and a small amount of a conformer of $\mathbf{N_{syn}}$ without the intramolecular hydrogen bond N···H−O, unable to undergo ESIPT and leading therefore to **N*** fluorescence upon excitation (Scheme 1). This conformer of $\mathbf{N_{syn}}$ must be planar, as its excitation spectrum was located at about the same position as that of the planar $\mathbf{N_{syn}}$ form. A similar planar rotamer unable to yield **T*** was detected for the parent compound HBI in protic solvents[21] and attributed to the anti rotamer $\mathbf{N_{anti}}$, with the phenol ring rotated 180° about the C2−C1′ bond. We suggest that a similar planar $\mathbf{N^*_{anti}}$ rotamer (Scheme 1) is responsible for the normal emission recorded for **1** and **2** at ~27 000 cm^{-1}.

In agreement with the proposed mechanism (Scheme 1), the fluorescence decay of **2** at 25 970 cm^{-1} (where only $\mathbf{N^*_{anti}}$ fluoresces) was monoexponential with a decay time of 1.29 ns (coincident with that of the **2-OMe** derivative), which must be due to $\mathbf{N^*_{anti}}$. Furthermore, between 25 000 and 21 740 cm^{-1}, the fluorescence decay was biexponential (Table 3), with a decay time of 1.28 ns and maximum contribution at high emission wavenumbers, due to $\mathbf{N^*_{anti}}$, and a second decay time of 0.65 ns, due to **T***, showing its maximum contribution at low wavenumbers. The fluorescence quantum yield of **T*** (0.09) was estimated by subtracting from the global emission spectrum the contribution of $\mathbf{N^*_{anti}}$ (its emission spectrum taken to be that of **2-OMe**) and assuming that at the excitation wavenumber only $\mathbf{N_{syn}}$ absorbs significantly. (Note that the absorption spectrum practically matched the excitation spectrum of the red-shifted fluorescence, attributed to $\mathbf{N_{syn}}$; see Figure 2b.)

The fluorescence spectra of **3** strongly depended on the excitation wavenumber (Figure 2c). Upon excitation at 31 250 cm^{-1}, we observed a single emission band, similar to the blue emission band detected for **2**, assigned to the normal form **N***. This suggests that **N*** is also the fluorescent species for compound **3**. Furthermore, excitation at 28 170 cm^{-1} (close to the maximum of the absorption spectrum) led to a very weak and broad red-shifted emission band, which must mainly correspond to **T***. The excitation spectrum recorded at the red edge of this emission spectrum (mainly due to **T***) was, except for a very weak contribution at 28 000 cm^{-1} (probably due to $\mathbf{N_{syn}}$), coincident with that monitored at 26 320 cm^{-1}, the maximum of **N*** emission. Moreover, these excitation spectra were about 2300 cm^{-1} blue-shifted with respect to the absorption spectrum. From these facts, we infer that a conformational equilibrium exists in the ground state for compound **3** in ethanol, like for **1** and **2**. However, the rotamer yielding the normal

SCHEME 2: Excitation and Deactivation Pathways of 3 in Ethanol[a]

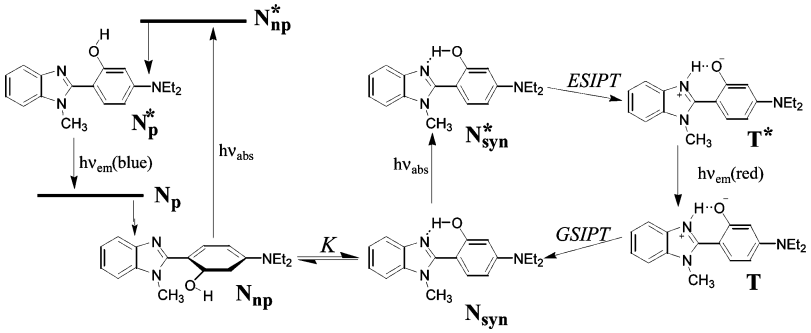

[a] The rotamer $\mathbf{N_{syn}}$ predominates in the ground state.

emission must be a nonplanar rotamer $\mathbf{N_{np}}$, because the blue shift of its excitation spectrum indicates a loss of electronic conjugation in this rotamer with respect to that in $\mathbf{N_{syn}}$, probably due to the steric hindrance of the methyl group and the solvated hydroxyl group. Furthermore, the fact that excitation of the nonplanar normal form of **3** led to an emission band very similar to that of the planar anti normal form of **1** and **2** (Figure 2) indicates that after excitation $\mathbf{N^*_{np}}$ rotates, reaching a planar conformation from which fluorescence takes place (Scheme 2). Also, for **3** the fluorescence quantum yield of **N*** must be much higher than that of **T***, because a strong fluorescence from **N*** (and a very weak one from **T***) was detected in spite of the fact that, according to the absorption spectrum, the rotamer $\mathbf{N_{syn}}$ predominates in the ground state.

Aqueous Solution. The absorption spectra of **1** and **2** in aqueous solution (Figures 3a and 3b) showed a new red-shifted band (band II) in addition to the usual band I observed in other solvents (Figures 1 and 2). The same behavior was found for the related molecules HBI,[21] HPyBI,[35] and HPyBO[8] and attributed to the existence in the ground state of the proton-transferred tautomeric form **T** in equilibrium with the normal form **N**. We propose that **1** and **2** exhibit in water a similar ground-state equilibrium between the tautomer **T**, responsible for absorption band II, and a normal form **N**, responsible for absorption band I. This interpretation is corroborated by the fact that the absorption spectrum of the O-methylated compound **2-OMe**, unable to form the tautomer, lacks band II. (Its absorption spectrum matches the excitation spectrum shown in Figure 3b.)

The fluorescent behavior of **1** and **2** in water (Figures 3a and 3b) was very similar except for the fact that upon excitation in absorption band II —due to **T**— no fluorescence of **T*** was detected for **2**, whereas a weak emission band, similar to that recorded in ethanol, was observed for **1**. Furthermore, excitation at ~33 000 cm^{-1} led to the emission spectrum of **N*** for compound **2** (it matched the emission band of **2-OMe**; Figure 3b) and to an emission spectrum mainly due to **N*** with a small contribution of **T*** for compound **1**. The excitation spectrum recorded at about the emission maximum of **N*** was for both compounds very similar to that recorded in ethanol (Figures 2a and 2b), previously attributed to $\mathbf{N_{anti}}$. This excitation spectrum matched the absorption spectrum of **1**, except in band II (due to **T**). This suggests that for compound **1** the absorption spectrum is only due to $\mathbf{N_{anti}}$ and **T**, no evidence of the presence of $\mathbf{N_{syn}}$ being found (Scheme 3). This interpretation is compatible with the fact that the excitation spectrum recorded for **1** at 21 280 cm^{-1} (close to the emission maximum of **T***) showed bands I and II, as we must take into account that the fluorescence from **N*** is much stronger than that of **T*** and is also detected at that emission wavenumber. In the case of compound **2**, the

SCHEME 3: Excitation and Deactivation Pathways of 1 (R = H) and 2 (R = C_2H_5) in Water

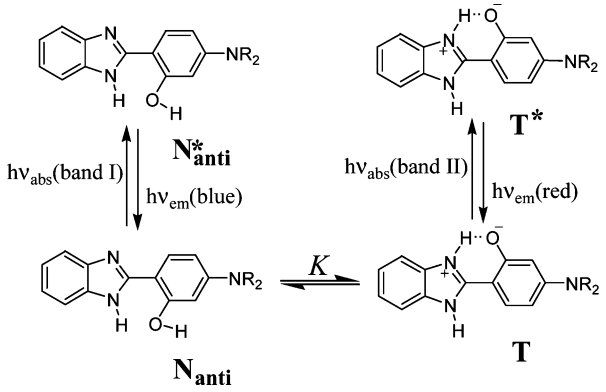

comparison between the excitation spectrum, due only to $\mathbf{N_{anti}}$, and the absorption spectrum, showing bands I and II (this due to **T**), allows us to conclude that, as for compound **1**, only $\mathbf{N_{anti}}$ and **T** are present in the ground state. Furthermore, in spite of the fact that no fluorescence band from **T*** was observed for **2** (no fluorescence could be recorded under excitation in band II), the time-resolved fluorescence measurements allowed **T*** to be detected. Whereas at 27 400 cm^{-1}, the fluorescence decay was monoexponential (Table 3) with a decay time of 1.53 ns, very close to that of **2-OMe** (1.44 ns; Table 2), due to the normal form, the fluorescence decay became biexponential at $\tilde{\nu}_{em} <$ 26 320 cm^{-1} with a decay time of about 1.65 ns, due to **N***, and another decay time of ~0.6 ns, due to **T***, mainly contributing to the global decay at low emission wavenumbers. According to this interpretation, we propose the mechanism of Scheme 3 to explain the behavior of **1** and **2** in aqueous solution.

The excitation and emission spectra of **3-OMe** in aqueous solution (Figure 3c) were both independent of the monitoring wavenumbers and very similar to the spectra recorded for this compound in cyclohexane (Figure 1a), and the excitation spectrum matched the absorption spectrum. This indicates that **3-OMe** behaves similarly in water and cyclohexane; that is, the excitation spectrum is due to the nonplanar normal form $\mathbf{N_{np}}$, which, as observed for compound **3** in ethanol (Scheme 2), planarizes upon excitation, yielding the emission spectrum of a planar normal form. The excitation and emission spectra of **3** in aqueous solution (Figure 3c) were almost the same as those recorded for the methoxy derivative **3-OMe**, except for a slight shift of the emission spectrum to the red on decreasing the excitation wavenumber. This suggests that the planar normal form is the main fluorescent species, its excitation spectrum corresponding to the nonplanar normal form $\mathbf{N_{np}}$. The absorption spectrum of **3** in aqueous solution was however very broad and strongly red-shifted with respect to the excitation spectrum. This

indicates that for **3** the major species present in the ground state is not $\mathbf{N_{np}}$ but another form absorbing to the red of the $\mathbf{N_{np}}$ spectrum. A close look at the absorption spectra of **1**, **2**, and **3** in aqueous solution (Figure 3) reveals that the spectrum of **3** showed an important contribution in the same region where absorption band II of **1** and **2** —attributed to **T**— was detected, this suggesting that **T** is also present in the ground state for **3**. The broadness of the absorption spectrum of **3** in aqueous solution makes it difficult to rule out the presence of $\mathbf{N_{syn}}$ in the ground state for this compound. However, as the expected amount of $\mathbf{N_{syn}}$ would be smaller for **3** than for **1** and **2**, due to the steric hindrance of the methyl group at the benzimidazole N1, and $\mathbf{N_{syn}}$ was not detected for the derivatives **1** and **2**, we conclude that compound **3** exhibits an equilibrium $\mathbf{N_{np}} \rightleftarrows \mathbf{T}$ in the ground state. This is in keeping with the fact that, whereas in neutral aqueous solution the parent molecule HBI showed an equilibrium in the ground state between $\mathbf{N_{syn}}$, $\mathbf{N_{anti}}$, and **T**,[21] its derivative **4**, with a methyl group at the benzimidazole N1, exists in the same solvent only as $\mathbf{N_{np}}$.[43] It is worth noting that the dialkylamino group at C4′ must stabilize the tautomer with respect to the normal form, as can be deduced from the fact that for **3** in water **T** is present in the ground state, whereas for its analogue **4**, without the diethylamino group at C4′, only the nonplanar form $\mathbf{N_{np}}$ was detected in that solvent.[43] The same conclusion is reached from the comparison of the relative absorption of **T** at band II in aqueous solution measured for **1**, **2**, and the parent compound HBI[21] under similar conditions, much higher for the amino derivatives. However, excitation of **3** at 28 170 cm^{-1}, where the absorption comes mainly from **T** and $\mathbf{N_{np}}$ hardly absorbs, led to the emission spectrum of the normal form except for a slight contribution from **T*** at low wavenumbers. This indicates that the fluorescence quantum yield of **T*** is extremely low in this solvent.

From these results, we conclude that the ground-state tautomeric and conformational equilibria of **1**, **2**, and **3** are modulated by the solvent. The normal forms $\mathbf{N_{anti}}$ (for **1** and **2**) and $\mathbf{N_{np}}$ (for **3**) and the tautomer **T** become much more stabilized than $\mathbf{N_{syn}}$ as the protic character of the solvent increases, $\mathbf{N_{syn}}$ being undetectable in aqueous solution for these compounds. Upon excitation of $\mathbf{N_{anti}}$ or $\mathbf{N_{np}}$, the fluorescence from the planar normal form is observed. Excitation of **T** leads to a very weak fluorescence from **T***, the fluorescence quantum yield decreasing on going from **1** to **2** and **3**. The reason for this difference in ϕ_T values will be discussed in section 2.

For the parent molecules HBI[21] and **4**,[43] excitation of $\mathbf{N_{anti}}$ (for HBI) or $\mathbf{N_{np}}$ (for **4**) in aqueous solution induced a rapid dissociation of these species at the hydroxyl group to yield the anion, no fluorescence from the neutral form being observed. A similar dissociation of the neutral form does not take place for the amino derivatives **2** and **3**. (Note that the emission spectra of the methoxy derivatives **2-OMe** and **3-OMe** (Figure 3), for which dissociation cannot take place, coincided with the emission spectra obtained for **2** and **3** under excitation of $\mathbf{N_{anti}}$.) Furthermore, for compound **1**, dissociation of the neutral form to give the anion (if it takes place) cannot be complete, as occurs for HBI, because the emission spectrum of the anion of **1** (data not shown) was different from that measured in neutral medium under excitation of $\mathbf{N_{anti}}$. The cause for the different photoacidities of HBI and **4** from those of their derivatives **1**, **2**, and **3** must be related to the presence of the dialkylamino group at C4′ position. Photodissociation of HBI (and in general that of phenols)[46] is induced by the increased electron-donor strength of the hydroxyl group and therefore the extent to which the electron density at the oxygen atom is conjugated with the aromatic ring in the excited state. For compounds **1**, **2**, and **3**, the electron conjugation of the dialkylamino group (a strong electron donor) decreases in part the electron-donor strength of the hydroxyl and therefore significantly decreases its excited-state acidity with respect to that observed for HBI and **4**.

Influence of Solvent and Temperature on the Tautomer Fluorescence for 1, 2, 3, and 4: Excited-State Proton-Coupled Charge-Transfer Takes Place. For HBI, the tautomer fluorescence quantum yield ϕ_T is independent of temperature (Figure 5a) and shows no dependence on the dielectric permittivity or viscosity of the solvent (Table 1). The behavior is completely different for the derivatives **2**, **3**, and **4**: Its tautomer fluorescence quantum yield decreases strongly on increasing the temperature (Figures 4 and 5), and the viscosity of the solvent (clearly observed for **2**) and the dielectric permittivity (more evident for **3**) appear to influence the values of ϕ_T. This suggests that for **2**, **3**, and **4** the excited tautomer experiences a solvent-dependent radiationless deactivation process that does not occur for HBI.

Some information about the tautomer radiationless deactivation can be obtained from the analysis of the temperature dependence of ϕ_T. For compounds **2**, **3**, and **4**, the fluorescence quantum yield of **T*** can be expressed as shown in eq 1. In this equation, k_f represents the fluorescence radiative constant, k_{conf} is the rate constant for the conformational change, and k_T represents the sum of all the radiative and nonradiative deactivation rate constants of **T***, except k_{conf}

$$\phi_T = \frac{k_f}{k_T + k_{conf}} \tag{1}$$

Assuming that k_{conf} is the only temperature-dependent deactivation rate constant and that k_{conf} shows an Arrhenius type dependence with temperature, $k_{conf} = A \exp(-E_{obs}/RT)$, eq 2 is derived, where ϕ_T^0 represents the fluorescence quantum yield of **T*** in the absence of any conformational change

$$\phi_T = \frac{\phi_T^0}{1 + (A/k_T)\exp(-E_{obs}/(RT))} \tag{2}$$

Furthermore, the observed activation energy E_{obs} is generally expressed[48] as given in eq 3

$$E_{obs} = E_a + \alpha E_\eta \tag{3}$$

In this equation, E_a is the intrinsic activation energy for the conformational motion, E_η is the solvent viscous-flow activation energy, and $0 < \alpha \leq 1$. According to eq 3, for a barrierless conformational change $E_{obs} \sim E_\eta$, whereas in the presence of an intrinsic activation energy $E_{obs} > E_\eta$.

Equation 2 fitted satisfactorily the experimental $\phi_T - T$ data obtained for compounds **2**, **3**, and **4** in diethyl ether and butyronitrile (Figure 5). The E_{obs} values obtained in diethyl ether (Table 4) were for the three compounds much higher than the corresponding E_η (7.095 kJ mol^{-1}),[49] this indicating that for these compounds the conformational change experienced by **T*** shows an intrinsic activation energy in this solvent. Furthermore, the value obtained for the fluorescence quantum yield of **T*** in the absence of any conformational motion, ϕ_T^0, was for **4** in diethyl ether (0.207) very similar to the fluorescence quantum yield of **T*** obtained for HBI (compound for which **T*** does not experience a thermally activated radiationless deactivation process) in various solvents (Table 1). Moreover, the values of ϕ_T^0 for compounds **2** (0.0859) and **3** (0.084) were very alike. It

TABLE 4: Parameters ϕ_T^0, A/k_T, and E_{obs}, Obtained by Fitting Eq 2 to the Experimental ϕ_T Values for 2, 3, and 4 in Various Solvents (Figure 5)

	value		
parameter	**4**	**2**	**3**
	Solvent: Diethyl Ether ($E_\eta = 7.095$ kJ mol^{-1})[a]		
ϕ_T^0	0.207 ± 0.007	0.0859 ± 0.0005	0.084 ± 0.009
A/k_T	$(1.1 \pm 0.8) \times 10^4$	$(1.2 \pm 0.2) \times 10^2$	$(2 \pm 2) \times 10^4$
E_{obs}/kJ mol^{-1}	18 ± 2	12.3 ± 0.4	15 ± 2
	Solvent: Butyronitrile ($E_\eta = 7.125$ kJ mol^{-1})[b]		
ϕ_T^0	0.2041 ± 0.0014		
A/k_T	$(3.0 \pm 0.2) \times 10^3$		
E_{obs}/kJ mol^{-1}	14.04 ± 0.13		

[a] Calculated from the viscosities of ref 49. [b] Calculated from the viscosities of ref 50.

is observed in Table 4 that the value of E_{obs} for **4** in butyronitrile (14.04 ± 0.13 kJ mol^{-1}) was higher than E_η of this solvent (7.125 kJ mol^{-1})[50] but lower than the observed activation energy obtained in diethyl ether (18 ± 2 kJ mol^{-1}). This suggests that the intrinsic activation barrier for the conformational change decreases when the solvent dielectric permittivity increases, because both solvents have about the same E_η value, but the dielectric permittivity of butyronitrile (24.8 at 25 °C)[51] is higher than that of diethyl ether (4.20 at 25 °C).[51]

We have already mentioned that for HBO and HBT, the benzoxazole and benzothiazole analogues of HBI, a thermally activated radiationless deactivation of **T***, associated with a large-amplitude conformational change, was detected. The published values of the activation energy of this process suggest that, also for these compounds, E_a decreases as the polarity of the solvent increases. Thus, the observed activation energy for HBO (15 kJ mol^{-1})[52] and HBT (16.2 kJ mol^{-1})[37] in 3-methylpentane was much higher than the activation energy of the viscous flow of 3-methylpentane (6.85 kJ mol^{-1}),[49] indicating that in this apolar solvent the conformational motion shows an intrinsic activation energy. In ethanol ($E_\eta = 13.25$ kJ mol^{-1}),[49] we found[8] $E_{obs} = E_\eta$ for HBT, whereas for HBO E_{obs} (17.5 kJ mol^{-1}) was slightly higher than E_η, this showing a much smaller activation energy for the conformational change in this polar solvent.

We have recently shown[8] that the conformational change experienced by the excited tautomer of HBO and HBT (and other derivatives) is connected to an intramolecular charge transfer taking place from the phenolate ring to the benzazolium moiety, the process being more efficient for the derivatives with a better donor−acceptor pair. If a similar charge-transfer process is the cause of the conformational change experienced by the excited tautomer of the compounds here studied, then the effectiveness of the radiationless deactivation process undergone by **T*** should be related to the efficiency of the redox pair present in **T***. The electron-donor ability of phenolate increases upon introduction of a $-NH_2$ group at C4′ (compound **1**) and further increases upon introduction at this position of a diethylamino group (compounds **2** and **3**), which would favor therefore the charge migration. Besides, if the large-amplitude conformational change experienced by the tautomer involves an internal rotation about the interannular bond, then N1-methylation should favor rotation and consequently the observation of the intramolecular charge-transfer process. In view of this, we would expect the efficiency of the radiationless deactivation process experienced by **T*** to increase in the series HBI < **2** < **3** due to the increase of electron-donor strength of the phenolate moiety on going from HBI to compound **2** and to the steric hindrance of the methyl group of **3**. This prediction is in keeping with the fact that in any solvent the fluorescence quantum yield of **T*** decreased in the order HBI (no conformational change) > **2** > **3**. With respect to compound **1**, we do not know if its tautomer undergoes a conformational change in the excited state, as the ϕ_T values could not be measured for this species. We can only say that, if that process occurs for **1**, then it must be less effective than that undergone by the tautomer of **2**, because under excitation of **T** in aqueous solution fluorescence from **T*** was observed for **1**, whereas it was not detected for **2**. In relation to compound **4**, the experimental result that the tautomer fluorescence quantum yield decreased in any solvent on going from HBI to **4** (Table 1) is also in agreement with the hypothesis that the steric hindrance of the methyl group favors an internal rotation associated with the intramolecular charge-transfer process.

It could be hypothesized that the temperature-dependent radiationless process detected for the N1-methylated derivative **4** might be related only with a geometric rearrangement favored by the steric hindrance, without the need for the intramolecular charge-transfer process. Evidence against this hypothesis comes from the different behavior observed for the N1-methylated derivatives of HBI and HPyBI. The fluorescence quantum yield of the N1-methylated derivative of HPyBI does not depend on the solvent (the maximum value was found in ethanol, $\phi = 0.45$, and the minimum value in acetonitrile, $\phi = 0.34$, the values for water and cyclohexane ranging in the middle)[46] and is very similar to that of the parent molecule HPyBI (values from 0.44 to 0.67 have been measured for this compound in various solvents).[35] The behavior is completely different for the N1-methylated derivative of HBI, **4**, which shows much lower quantum yields than HBI and a greater dependence on the solvent (Table 1). These results provide evidence for the decisive influence of the electron-donor strength of the donor moiety on the radiationless deactivation. As the dissociated pyridinol is a worse electron donor than the dissociated phenol,[8] an effective radiationless deactivation is observed for the tautomer of **4** but not for the N1-methylated derivative of HPyBI.

The efficiency of the charge-transfer processes is known to increase with the solvent polarity[53] due to the stabilization of a more polar charge-transfer (CT) state, which causes the intrinsic activation energy to decrease. The decrease of ϕ_T (and consequently higher efficiency of the CT process) observed for **3** on increasing the solvent dielectric permittivity (Table 1) is in keeping with this. We have also shown in previous paragraphs that for compounds **4** (Table 4), HBO,[52] and HBT[37] the activation energy for the radiationless deactivation process of **T*** decreases on increasing the solvent polarity. The effect of the solvent dielectric permittivity on the CT process is not so clear for **2**, which shows a smooth increase of ϕ_T with viscosity,

SCHEME 4: Excited-State Coupled Intramolecular Proton and Charge Transfer of 2 (X = NH), 3 (X = NMe), and 4[a]

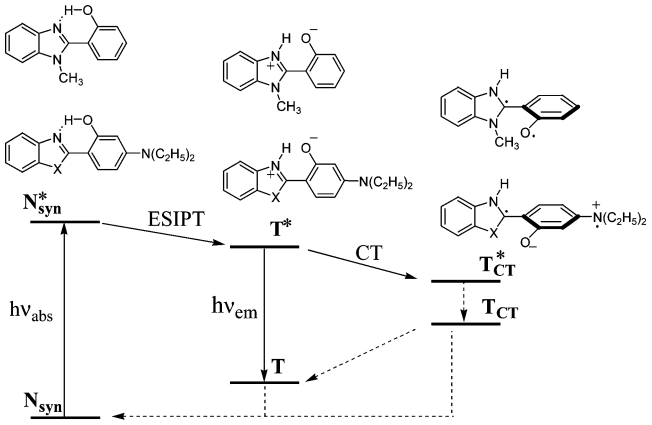

[a] The real structure of the T^*_{CT} species is unkown.

independently of the dielectric permittivity of the solvent (Table 1). This may imply a lower polarity of the CT state for this compound.

From the above considerations, we propose that compounds **2**, **3**, and **4** in nonaqueous solvents undergo an excited-state coupled proton and electron transfer depicted in Scheme 4. Upon excitation of $\mathbf{N_{syn}}$, an ESIPT process to give **T*** takes place, after which the excited tautomer undergoes a large-amplitude conformational change associated with a charge migration from the deprotonated dialkylamino phenol ring to the protonated benzimidazole, yielding the nonfluorescent charge-transfer intermediate $\mathbf{T^*_{CT}}$, which probably deactivates very fast.[8] The ground-state mechanism by which $\mathbf{N_{syn}}$ regenerates has not been studied here. It is worth noting that we do not have any information about the real structure of the charge-transfer intermediate. The electronic and geometric structure of $\mathbf{T^*_{CT}}$ shown in Scheme 4 is hypothetical, not only about the nature of the conformational change experienced by **T*** but also in relation to the charge distribution (several resonance forms exist not only for $\mathbf{T^*_{CT}}$ but also for **T***, which can be written in ketonic structure without formal charges; see Chart 1).

Conclusions

In this article, we have studied the ground- and excited-state behavior of the novel compounds 2-(4′-amino-2′-hydroxyphenyl)benzimidazole (**1**), 2-(4′-*N*,*N*-diethylamino-2′-hydroxyphenyl)benzimidazole (**2**), and 1-methyl-2-(4′-*N*,*N*-diethylamino-2′-hydroxyphenyl)benzimidazole (**3**) in various solvents. We have shown that for these compounds there is a solvent-modulated rotameric and tautomeric equilibrium in the ground state. In cyclohexane, these compounds mainly exist in the ground state as the planar syn normal form $\mathbf{N_{syn}}$, with the hydroxyl group hydrogen-bonded to the benzimidazole N3. In ethanol, the $\mathbf{N_{syn}}$ form is in equilibrium with its planar anti rotamer $\mathbf{N_{anti}}$, for **1** and **2**, and with a nonplanar $\mathbf{N_{np}}$ rotamer for **3**. In contrast to the behavior of HBI, which showed in aqueous solution an equilibrium between $\mathbf{N_{syn}}$, $\mathbf{N_{anti}}$, and **T**, for the dialkylamino derivatives **1** and **2** the rotamer $\mathbf{N_{syn}}$ was not detected in aqueous solution, an equilibrium between $\mathbf{N_{anti}}$ and **T** being observed for these compounds. Similarly, whereas for **4** only $\mathbf{N_{np}}$ was detected in aqueous solution, for its analogue **3** the nonplanar normal form is in equilibrium with **T**. Our results showed that the dialkylamino group in the phenolic moiety of **1**, **2**, and **3** favors the existence of tautomer **T** in the ground state in aqueous solution.

Upon excitation of $\mathbf{N_{syn}}$, this form undergoes for **1**, **2**, and **3** an ESIPT process to yield **T***, fluorescence from **T*** being detected. Direct excitation of **T** in aqueous solution led to a weak **T*** emission for **1**, fluorescence from **T*** being hardly detected for **2** and **3**.

Whereas the fluorescence quantum yield and lifetime of **T*** showed for HBI no dependence on solvent or temperature, those of the tautomers of **2**, **3**, and **4** revealed a temperature-, polarity-, and viscosity-dependent radiationless deactivation connected with a large-amplitude conformational motion occurring for these HBI derivatives. We have shown that, as recently reported by us for HBO, HBT, and other hydroxyarylbenzazoles, this conformational change is associated with a charge-transfer experienced by **T*** from the deprotonated dialkylaminophenol or phenol (donor) to the protonated benzimidazole (acceptor), affording a nonfluorescent charge-transfer tautomer $\mathbf{T^*_{CT}}$. The efficiency of this intramolecular charge-transfer process, not observed for HBI, increased with the electron-donor strength and with the steric hindrance caused by N1-methylation and decreased as the solvent viscosity was increased. These compounds are examples of molecules undergoing excited-state intramolecular coupled proton and electron transfer.

Acknowledgment. We thank the Spanish Ministry of Education and Science, and the European Regional Development Fund (Project No. CTQ 2004-07683-C02-01/BQU), and the Xunta de Galicia (DXID, Project No. PGIDIT05PXIC20905PN) for financial support of this work.

References and Notes

(1) Cukier, R. I.; Nocera, D. G. *Annu. Rev. Phys. Chem.* **1998**, *49*, 337.
(2) Llano, J.; Eriksson, L. A. *Phys. Chem. Chem. Phys.* **2004**, *6*, 2426.
(3) Perun, S.; Sobolewski, A. L.; Domcke, W. *J. Phys. Chem. A* **2006**, *110*, 9031.
(4) Sobolewski, A. L.; Domcke, W. *ChemPhysChem* **2006**, *7*, 561.
(5) Faxen, K.; Gilderson, G.; Aedelroth, P.; Brzezinski, P. *Nature* **2005**, *437*, 286.
(6) Belevich, I.; Verkhovsky, M. I.; Wikstroem, M. *Nature* **2006**, *440*, 829.
(7) Crofts, A. R. *Biochim. Biophys. Acta* **2004**, *1655*, 77.
(8) Vazquez, S. R.; Rodriguez, M. C. R.; Mosquera, M.; Rodriguez-Prieto, F. *J. Phys. Chem. A* **2007**, *111*, 1814.
(9) Formosinho, S. J.; Arnaut, L. G. *J. Photochem. Photobiol., A* **1993**, *75*, 21.
(10) Ormson, S. M.; Brown, R. G. *Prog. React. Kinet.* **1994**, *19*, 45.
(11) Paterson, M. J.; Robb, M. A.; Blancafort, L.; DeBellis, A. D. *J. Phys. Chem. A* **2005**, *109*, 7527.
(12) Lim, S.-J.; Seo, J.; Park, S. Y. *J. Am. Chem. Soc.* **2006**, *128*, 14542.
(13) Klymchenko, A. S.; Pivovarenko, V. G.; Demchenko, A. P. *J. Phys. Chem. A* **2003**, *107*, 4211.
(14) Gaenko, A. V.; Devarajan, A.; Tselinskii, I. V.; Ryde, U. *J. Phys. Chem. A* **2006**, *110*, 7935.
(15) Waluk, J. *Conformational Analysis of Molecules in Excited States*; Wiley-VCH: New York, 2000.
(16) Williams, D. L.; Heller, A. *J. Phys. Chem.* **1970**, *74*, 4473.
(17) Sinha, H. K.; Dogra, S. K. *Chem. Phys.* **1986**, *102*, 337.
(18) Das, K.; Sarkar, N.; Ghosh, A. K.; Majumdar, D.; Nath, D. N.; Bhattacharyya, K. *J. Phys. Chem.* **1994**, *98*, 9126.
(19) Das, K.; Sarkar, N.; Majumdar, D.; Bhattacharyya, K. *Chem. Phys. Lett.* **1992**, *198*, 443.
(20) Douhal, A.; Amat-Guerri, F.; Lillo, M. P.; Acuna, A. U. *J. Photochem. Photobiol., A* **1994**, *78*, 127.
(21) Mosquera, M.; Penedo, J. C.; Rios Rodriguez, M. C.; Rodriguez-Prieto, F. *J. Phys. Chem.* **1996**, *100*, 5398.
(22) Rios, M. A.; Rios, M. C. *J. Phys. Chem. A* **1998**, *102*, 1560.
(23) Wang, H.; Zhang, H.; Abou-Zied, O. K.; Yu, C.; Romesberg, F. E.; Glasbeek, M. *Chem. Phys. Lett.* **2002**, *367*, 599.
(24) Abou-Zied, O. K.; Jimenez, R.; Thompson, E. H. Z.; Millar, D. P.; Romesberg, F. E. *J. Phys. Chem. A* **2002**, *106*, 3665.
(25) Arthen-Engeland, T.; Bultmann, T.; Ernsting, N. P.; Rodriguez, M. A.; Thiel, W. *Chem. Phys.* **1992**, *163*, 43.
(26) Rios, M. A.; Rios, M. C. *J. Phys. Chem.* **1995**, *99*, 12456.

(27) Fernandez-Ramos, A.; Rodriguez-Otero, J.; Rios, M. A.; Soto, J. *J. Mol. Struct.: THEOCHEM* **1999**, *489*, 255.
(28) Lochbrunner, S.; Stock, K.; Riedle, E. *J. Mol. Struct.* **2004**, *700*, 13.
(29) Barbara, P. F.; Brus, L. E.; Rentzepis, P. M. *J. Am. Chem. Soc.* **1980**, *102*, 5631.
(30) Elsaesser, T.; Schmetzer, B.; Lipp, M.; Baeuerle, R. J. *Chem. Phys. Lett.* **1988**, *148*, 112.
(31) Laermer, F.; Elsaesser, T.; Kaiser, W. *Chem. Phys. Lett.* **1988**, *148*, 119.
(32) Frey, W.; Laermer, F.; Elsaesser, T. *J. Phys. Chem.* **1991**, *95*, 10391.
(33) Lochbrunner, S.; Wurzer, A. J.; Riedle, E. *J. Phys. Chem. A* **2003**, *107*, 10580.
(34) Rini, M.; Kummrow, A.; Dreyer, J.; Nibbering, E. T. J.; Elsaesser, T. *Faraday Discuss.* **2002**, *122*, 27.
(35) Rodriguez Prieto, F.; Rios Rodriguez, M. C.; Mosquera Gonzalez, M.; Rios Fernandez, M. A. *J. Phys. Chem.* **1994**, *98*, 8666.
(36) Brewer, W. E.; Martinez, M. L.; Chou, P. T. *J. Phys. Chem.* **1990**, *94*, 1915.
(37) Al-Soufi, W.; Grellmann, K. H.; Nickel, B. *Chem. Phys. Lett.* **1990**, *174*, 609.
(38) Chou, P. T.; Martinez, M. L.; Studer, S. L. *Chem. Phys. Lett.* **1992**, *195*, 586.
(39) Stephan, J. S.; Grellmann, K. H. *J. Phys. Chem.* **1995**, *99*, 10066.
(40) Nagaoka, S.; Itoh, A.; Mukai, K.; Nagashima, U. *J. Phys. Chem.* **1993**, *97*, 11385.
(41) Ikegami, M.; Arai, T. *J. Chem. Soc., Perkin Trans. 2* **2002**, 1296.
(42) Becker, R. S.; Lenoble, C.; Zein, A. *J. Phys. Chem.* **1987**, *91*, 3509.
(43) Rodriguez-Prieto, F.; Penedo, J. C.; Mosquera, M. *J. Chem. Soc., Faraday Trans.* **1998**, *94*, 2775.
(44) Melhuish, W. H. *J. Phys. Chem.* **1961**, *65*, 229.
(45) Crosby, G. A.; Demas, J. N. *J. Phys. Chem.* **1971**, *75*, 991.
(46) Ríos Rodríguez, M. C.; Rodríguez-Prieto, F.; Mosquera, M. *Phys. Chem. Chem. Phys.* **1999**, *1*, 253.
(47) Ireland, J. F.; Wyatt, P. A. H. *Adv. Phys. Org. Chem.* **1976**, *12*, 131.
(48) Rettig, W.; Fritz, R.; Braun, D. *J. Phys. Chem. A* **1997**, *101*, 6830.
(49) Lax, E. *Taschenbuch für Chemiker und Physiker: Makroskopische Physikalisch-Chemische Eigenschaften.*; Springer-Verlag: Berlin, 1967.
(50) Harju, T. O.; Korppi-Tommola, J. E. I.; Huizer, A. H.; Varma, C. A. G. O. *J. Phys. Chem.* **1996**, *100*, 3592.
(51) Marcus, Y. *The Properties of Solvents*; John Wiley & Sons: Chichester, U. K., 1998.
(52) Mordzinski, A.; Grellmann, K. H. *J. Phys. Chem.* **1986**, *90*, 5503.
(53) Grabowski, Z. R.; Rotkiewicz, K.; Rettig, W. *Chem. Rev.* **2003**, *103*, 3899.
(54) Lide, D. R. *Handbook of Chemistry and Physics: A Ready Reference of Chemical and Physical Data*, 85th ed.; CRC Press: Boca Raton, FL, 2004.